ENHANCED INTERFERENCE SUPPRESSION FOR SPECTRUM-EFFICIENT HIGH DATA-RATE TRANSMISSIONS OVER WIDEBAND CDMA NETWORKS

Sofiène AFFES[1], *Karim CHEIKHROUHOU*[2], *and Paul MERMELSTEIN*[1]

1: INRS-Télécommunications, Université du Québec
800, de la Gauchetière Ouest, Suite 6900, Montréal, Québec, H5A 1K6, Canada
2: École Nationale d'Ingénieurs de Tunis, BP 37, Le Belvédère , Tunis, 1002, Tunisia

ABSTRACT

Recently we developed an efficient multiuser upgrade of the single-user spatio-temporal array-receiver (STAR), referred to as interference subspace rejection (ISR). The resulting STAR-ISR receiver offers a number of implementation modes covering a large range in performance and complexity for wideband CDMA networks. Here we apply STAR-ISR to high data-rate (HDR) transmissions by extending operation to delay spreads larger than the symbol duration. Low processing gain situations render symbol timing extremely difficult, especially with RAKE-type receivers. For HDR links of 512 Kbps in 5 MHz bandwidth, simulations indicate that the simplest mode of STAR-ISR outperforms the 2D-RAKE-PIC by factor 4 to 5 in spectrum efficiency while requiring the same order of complexity. This gain increases up to factor 7.5 in high Doppler.

1. INTRODUCTION

We have recently proposed a unifying framework for a new class of receivers that employ linearly-constrained interference cancellation for multiuser detection in wideband CDMA [1]. These detectors referred to as ISR operate in multiple mixed-traffic scenarios and in various modes, ranging in performance and complexity from linear receivers to interference cancellers. In addition to interference rejection, they perform space and time diversity combining, array processing and synchronization using STAR [2].

So far, however, we investigated the STAR-ISR receiver solutions with delay spreads smaller in chips than the processing gain. HDR applications require spreading factors smaller than the delay spread. These low processing gain situations render symbol timing extremely difficult. More importantly, they see inter-symbol interference (ISI) and inter-path interference (IPI) increase dramatically to the point of seriously deteriorating the receiver performance. From 3G wideband radio-channel models [3], we made an assessment that current synchronization techniques cannot achieve satisfactory performance with processing gains below 32 (see high-rate example in [2]). A review of the recent literature on synchronization in wideband CDMA receivers confirms this limitation. The proposed HSDPA standard [3] exemplifies this limit. The 32 minimum spreading factor limit there sets a bound on the peak rate achievable with BPSK. It hence suggests use of higher-order modulations to increase the peak rate up to 540 Kbps per spreading code with 64-QAM.

Similarly, we are investigating use of higher-order modulations [4]. However, increase in the transmission rate with more power-efficient lower-order modulations such as BPSK or QPSK offers an even more promising path for achieving substantial gains both in peak rate and spectrum efficiency. Accordingly, we propose a HDR implementation that operates STAR-ISR at processing gains lower than 32.

The HSDPA standard considers implementation of PIC, but leaves open all issues related to synchronization and channel identification [3]. Yet despite reports on the challenging problems met when operating RAKE-type receivers in HDR applications [3],[5], the 2D-RAKE-PIC is currently accepted as the best receiver candidate for implementation to our knowledge [5],[6]. In this work, we develop an enhanced HDR implementation of the 2D-RAKE-PIC as a reference. For HDR links of 512 Kbps in 5 MHz bandwidth, simulations indicate that the simplest mode of STAR-ISR outperforms the 2D-RAKE-PIC by factor 4 to 7.5 in spectrum efficiency while requiring the same complexity.

2. DATA MODEL AND FORMULATION

We consider the uplink of an asynchronous cellular CDMA system where each base-station is equipped with M receiving antennas. All desired users in a served cell or sector, *NI* in number, transmit with the same BPSK modulation and at the same rate $1/T$. The BPSK sequence $b^i(t)$ of a desired user with index $i \in \{1, \dots, NI\}$ is spread by a long personal PN code $c^i(t)$ at a rate $1/T_c$, where T_c is the chip pulse duration. The processing gain is given by $L = T/T_c$. Finally, we assume a multipath Rayleigh fading environment with P resolvable paths with a delay spread $\Delta\tau$. $N_f = MP$ hence denotes the total number of diversity fingers.

In contrast to [1],[2], here we no longer require that the delay spread be small compared to the symbol duration (*i.e.*, $\Delta\tau \ll T$), a very limiting assumption indeed in the HDR case where very likely $\Delta\tau > T$. Similarly to [2], we define the enlarged delay-spread $\overline{\Delta\tau} > \Delta\tau$ to allow an increased uncertainty margin (*i.e.*, $T < \Delta\tau < \overline{\Delta\tau}$) for the tracking of time-varying multipaths due to clock drifts and receiver mobility. We also define $L_{\overline{\Delta}} = \lceil \overline{\Delta\tau}/T_c \rceil$ and $Q_{\overline{\Delta}} = \lceil \overline{\Delta\tau}/T \rceil$ the corresponding lengths in chip samples and symbols, respectively.

After chip-pulse matched-filtering, sampling at the chip rate and framing over $QL+L_{\overline{\Delta}}$ chip samples at the processing rate $1/T_P$ where $T_P = QT$ denotes the block processing period, we obtain the $M \times (QL+L_{\overline{\Delta}})$ matched-filtering observation matrix for the n-th block (see details in [1]):

$$\mathbf{Y}_n = [Y_n(0), Y_n(T_c), \ldots, Y_n((QL + L_{\overline{\Delta}} - 1)T_c)] \ . \quad (1)$$

Defining for convenience of notation a vector $\mathbb{Y}$ as a matrix $\mathbf{Y}$ reshaped column-wise, we rewrite the vectorized matched-filtering observation matrix $\mathbf{Y}_n$ of Eq. (1) with respect to the k-th symbol ($k = 0, \ldots, Q-1$) of the i-th desired user ($i = 1, \ldots, NI$) as:

$$\begin{aligned} \mathbb{Y}_n &= \psi_n^i b_{nQ+k}^i \mathbb{Y}_{k,n}^i + \left\{ \psi_n^i \mathbb{I}_{\text{ISI},n}^{i,k} + \sum_{\substack{i'=1 \\ i' \neq i}}^{NI} \psi_n^{i'} \mathbb{Y}_n^{i'} \right\} + \mathbb{N}_n \\ &= s_n^{i,k} \mathbb{Y}_{k,n}^i + \mathbb{I}_n^{i,k} + \mathbb{N}_n \ , \end{aligned} \quad (2)$$

where for the i-th user at the n-th data block $b_{nQ+k}^i = b^i((nQ+k)T)$, $s_n^{i,k} = \psi_n^i b_{nQ+k}^i$ is the k-th signal component, $\mathbb{Y}_{k,n}^i$ is the canonic user-observation vector of the k-th symbol, $\mathbb{Y}_n^i$ is the user-observation vector and $\mathbb{I}_{\text{ISI},n}^{i,k} = \mathbb{Y}_n^i - b_{nQ+k}^i \mathbb{Y}_{k,n}^i$ is the ISI vector over the the k-th symbol [1]. $\mathbb{I}_n^{i,k}$, referred to as the interference vector in the following, denotes the part of the multiple access interference (MAI) vector to be suppressed, including ISI from user i over its k-th symbol. The noise vector $\mathbb{N}_n$ comprises the rest of the MAI from all other users in the system and the preprocessed thermal noise [1].

Provided that the data block edges are properly positioned after time acquisition, the parametric data decompositions introduced in [1] detail the structure of the interference vector as follows:

$$\mathbb{I}_n^{i,k} = \sum_{i'=1}^{NI} \sum_{f=1}^{N_f} \sum_{k'=-Q_{\overline{\Delta}}}^{Q+Q_{\overline{\Delta}}-1} \psi_n^{i'} \zeta_{f,n}^{i'} b_{nQ+k}^{i'} \mathbb{Y}_{k',n}^{i',f} \bar{\delta}_{i',i}^{k',k} \ , \quad (3)$$

where finger $f = (p-1)M + m \in \{1, \ldots, N_f\}$, denotes antenna $m \in \{1, \ldots, M\}$ and propagation path $p \in \{1, \ldots, P\}$, $\zeta_{f,n}^u$ stands for the corresponding propagation coefficient, $\mathbb{Y}_{k,n}^{u,f}$ is the canonic diversity-observation vector

ISR Mode	$\hat{\mathbf{C}}_n^{i,k} = \left[\ldots, \hat{\mathbb{C}}_{j,n}^{i,k}, \ldots \right]$
TR	$\left[\sum_{i'=1}^{NI} \sum_{f=1}^{N_f} \sum_{k'=-Q_{\overline{\Delta}}}^{Q+Q_{\overline{\Delta}}-1} \hat{\psi}_n^{i'} \hat{\zeta}_{f,n}^{i'} \hat{b}_{nQ+k}^{i'} \hat{\mathbb{Y}}_{k',n}^{i',f} \bar{\delta}_{i',i}^{k',k} \right]$ $\Rightarrow N_c = 1$
R	$\left[\ldots, \sum_{f=1}^{N_f} \sum_{k'=-Q_{\overline{\Delta}}}^{Q+Q_{\overline{\Delta}}-1} \hat{\zeta}_{f,n}^{i'} \hat{b}_{nQ+k}^{i'} \hat{\mathbb{Y}}_{k',n}^{i',f} \bar{\delta}_{i',i}^{k',k}, \ldots \right]$ $\Rightarrow N_c = NI$
D	$\left[\ldots, \sum_{k'=-Q_{\overline{\Delta}}}^{Q+Q_{\overline{\Delta}}-1} \hat{b}_{nQ+k}^{i'} \hat{\mathbb{Y}}_{k',n}^{i',f} \bar{\delta}_{i',i}^{k',k}, \ldots \right]$ $\Rightarrow N_c = N_f NI$
H	$\left[\ldots, \sum_{f=1}^{N_f} \hat{\zeta}_{f,n}^{i'} \hat{\mathbb{Y}}_{k',n}^{i',f} \bar{\delta}_{i',i}^{k',k}, \ldots \right]$ $\Rightarrow N_c = (Q + 2Q_{\overline{\Delta}})NI$

Tab. 1. The signal blocking matrix $\hat{\mathbf{C}}_n^{i,k}$ and the corresponding number of constraints or columns N_c for each ISR mode. Each generic column $\hat{\mathbb{C}}_{j,n}^{i,k}$ shown above is divided by the norm of the corresponding generic column $\hat{\mathbb{C}}_{j,n}$ of the constraint matrix $\hat{\mathbf{C}}_n$ (obtained here by replacing $\bar{\delta}_{i',i}^{k',k}$ with 1).

[1], and $\bar{\delta}_{i',i}^{k',k} = 0$ if $i' = i$ and $k' = k$, and 1 otherwise. The resulting parametric decompositions of interference in Eq. (3) for large delay-spread situations give rise to the following HDR implementation of STAR-ISR.

3. HDR IMPLEMENTATION OF STAR-ISR

3.1. HDR Symbol Estimation with ISR

Using joint ISR detection [1], we extract the k-th symbol ($k = 0, \ldots, Q-1$) of the i-th desired user ($i = 1, \ldots, NI$) with the following combiner:

$$\mathbb{W}_n^{i,k} = \frac{\Pi_n^{i,k} \hat{\mathbb{Y}}_{k,n}^i}{\hat{\mathbb{Y}}_{k,n}^{i\,H} \Pi_n^{i,k} \hat{\mathbb{Y}}_{k,n}^i} = \Pi_n^{i,k} \frac{\hat{\mathbb{Y}}_{k,n}^i}{\|\hat{\mathbb{Y}}_{k,n}^i\|^2} = \Pi_n^{i,k} \mathbb{W}_{\text{MRC},n}^{i,k}, \quad (4)$$

where $\Pi_n^{i,k} = \mathbf{I}_{N_T} - \hat{\mathbf{C}}_n \mathbf{Q}_n \hat{\mathbf{C}}_n^{i,k\,H}$ is a projection orthogonal to the interference vector $\mathbb{I}_n^{i,k}$ in the observation space of dimension $N_T = M(QL + L_{\overline{\Delta}})$. $\hat{\mathbf{C}}_n$ and $\hat{\mathbf{C}}_n^{i,k}$ denote the constraint matrix and the corresponding signal blocking matrix, respectively [1].

It is in the constraint matrices of Tab. 1 that we observe the modifications required for large delay-spreads in HDR applications. Indeed in the DF (decision feedback) modes, construction of the constraint matrices requires now estimation of $Q_{\overline{\Delta}}$ past symbols from the previous data block (with ISR combining) as well as estimation of $Q_{\overline{\Delta}}$ future symbols from the next data block (with simple MRC) [1]. To complete construction of the constraint matrices, the Q target symbols in the current data block are estimated in an initial stage with MRC (*i.e.*, stage 0) [1]. Once the constraint matrices are available, the target symbols are reestimated with ISR combining. This process is repeated iteratively in a multistage structure and terminated say after N_s stages [1]. In the H mode, however, neither decision feedback nor processing delays are required but the number of constraints N_c increases from $(Q+2)NI$ for small delay spreads [1] to $(Q+2Q_{\overline{\Delta}})NI$ in Tab. 1.

ISR combining in Eq. (4) is actually implemented in cascade, first by projection of the matched-filtering observation vector to yield the new observation:

$$\underline{\mathrm{Y}}_{\Pi,n}^{i,k} = \Pi_n^{i,k} \underline{\mathrm{Y}}_n \,, \tag{5}$$

then by coherent MRC combining to estimate the k-th signal component of the i-th user as follows (see Eq. (4)):

$$\hat{s}_n^{i,k} = \mathrm{Real}\left\{ \underline{\mathrm{W}}_{\mathrm{MRC},n}^{i,k\,H} \underline{\mathrm{Y}}_{\Pi,n}^{i,k} \right\} \,. \tag{6}$$

Taking the sign of the signal components above allows estimation of the BPSK symbols $\hat{b}_{nQ+k}^{i}$ for $k = 0, \ldots, Q-1$ and for $i = 1, \ldots, NI$.

3.2. HDR Channel Identification with STAR

Note that the new observation $\underline{\mathrm{Y}}_{\Pi,n}^{i,k}$ is almost interference-free (in the sense that any contribution from the interference vector $\underline{\mathrm{I}}_n^{i,k}$ is rejected). By despreading its matrix-reshaped form $\mathbf{Y}_{\Pi,n}^{i,k}$, defined as

$$\mathbf{Y}_{\Pi,n}^{i,k} = \left[Y_{\Pi,n}^{i,k}(0), \ldots, Y_{\Pi,n}^{i,k}((QL + L_{\overline{\Delta}} - 1)T_c) \right] \,, \tag{7}$$

with the code segment that spreads the k-th symbol of the i-th user, we obtain the following $M \times L_{\overline{\Delta}}$ reduced-size postcorrelation matrix [2]:

$$\mathbf{Z}_{\Pi,n}^{i,k} = \left[Z_{\Pi,n}^{i,k}(0), \ldots, Z_{\Pi,n}^{i,k}((L_{\overline{\Delta}} - 1)T_c) \right] \,, \tag{8}$$

where for $l = 0, \ldots, L_{\overline{\Delta}} - 1$:

$$Z_{\Pi,n}^{i,k}(lT_c) = \frac{1}{L} \sum_{l'=0}^{L-1} Y_n((kL + l + l')T_c) c_{nQ+k,l'}^{i} \,, \tag{9}$$

and for $l' = 0, \ldots, L-1$, $c_{n,l'}^{i} = \pm 1$ is the l'-th chip of the spreading-code segment over the n-th period T. The resulting vector-reshaped postcorrelation vector is also almost interference-free and has the following structure [7]:

$$\underline{\mathrm{Z}}_{\Pi,n}^{i,k} \simeq s_n^{i,k} \underline{\mathrm{H}}_n^{i} + \underline{\mathrm{N}}_{\mathrm{PCM},n}^{i,k} \,, \tag{10}$$

where $\underline{\mathrm{H}}_n^{i}$ denotes the $ML_{\overline{\Delta}} \times 1$ spatio-temporal propagation vector of the i-th user [1],[2] and $\underline{\mathrm{N}}_{\mathrm{PCM},n}^{i,k}$ is the postcorrelation noise vector obtained by projection and despreading of the spatio-temporal noise vector $\underline{\mathrm{N}}_n$ of Eq. (2).

The expression for the new postcorrelation vector $\underline{\mathrm{Z}}_{\Pi,n}^{i,k}$ in Eq. (10) approaches that of a single-user observation if $\underline{\mathrm{N}}_{\mathrm{PCM},n}^{i,k}$ is approximated as an uncorrelated spatio-temporal noise vector. It allows implementation of STAR in a single-user structure by exploiting the advantages of ISR in the so-called decision feedback identification procedure (DFI) [2] with projection (Π-DFI) proposed in [7]. We adapt it below to HDR applications.

We exploit the fact that the channel parameters are assumed constant over the processing period T_P (as reflected in Eq. (10) where the channel $\underline{\mathrm{H}}_n^{i}$ is indeed identical for all Q target symbols) to update the estimate of the propagation vector $\hat{\underline{\mathrm{H}}}_n^{i}$ at the processing rate using the following block Π-DFI procedure:

$$\hat{\underline{\mathrm{H}}}_{n+1}^{i} = \hat{\underline{\mathrm{H}}}_n^{i} + \frac{\mu}{Q} \sum_{k=0}^{Q-1} \left(\underline{\mathrm{Z}}_{\Pi,n}^{i,k} - \hat{\underline{\mathrm{H}}}_n^{i} \hat{s}_n^{i,k} \right) \hat{s}_n^{i,k\,*} \,, \tag{11}$$

where μ denotes the adaptation step-size.

4. EVALUATION AND CONCLUSIONS

We consider here the simplest ISR mode TR (see Tab. 1) for performance assessment of four versions of the STAR-ISR receiver and consider as a reference a combination of multistage PIC with the enhanced 2D-RAKE version with the early-late gate developed in [2]. In the first STAR-ISR HDR version simply referred to as STAR-ISR-TR, we deactivate the new block Π-DFI procedure and use instead simple DFI (*i.e.*, ISR advantages through projection of the observation before despreading [7] are not exploited). We also use the default ISR structure with $N_s = 1$ stage [1]. In the second version referred to as STAR-ISR-TR-Π, we activate the new block Π-DFI procedure. In the third version referred to as STAR-ISR-TR-M(2), we implement the multistage option of ISR with $N_s = 2$ stages. In the fourth and last version referred to as STAR-ISR-TR-Π-M(2), we activate both the new block Π-DFI procedure and the multistage option of ISR with $N_s = 2$ stages. In the reference 2D-RAKE-PIC-M(2) HDR implementation, we always use $N_s = 2$ stages.

For simulations, we select a wideband CDMA system of 4.096 Mcps, HDR links at 512 Kbps (*i.e.*, $L = 8$) after channel coding (or for instance 256 Kbps with rate-1/2 channel coding), $Q = 8$ symbols/block, $M = 2$ antennas, $P = 3$ equal-power fading paths, a delay spread $\Delta\tau = 8$ chips and an enlarged delay-spread $L_{\overline{\Delta}} = 32$ chips (*i.e.* larger than

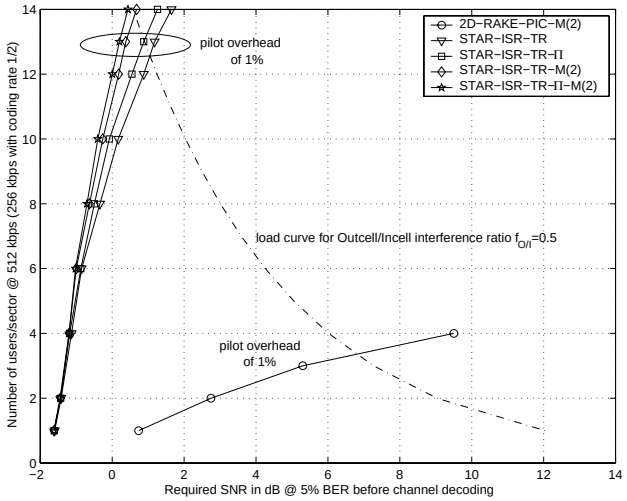

Fig. 1. Required SNR at a BER of 5% before FEC decoding vs. the number of users per cell or sector *NI* for STAR-ISR-TR and the 2D-RAKE-PIC-M(2) (*i.e.*, $N_s = 2$ stages).

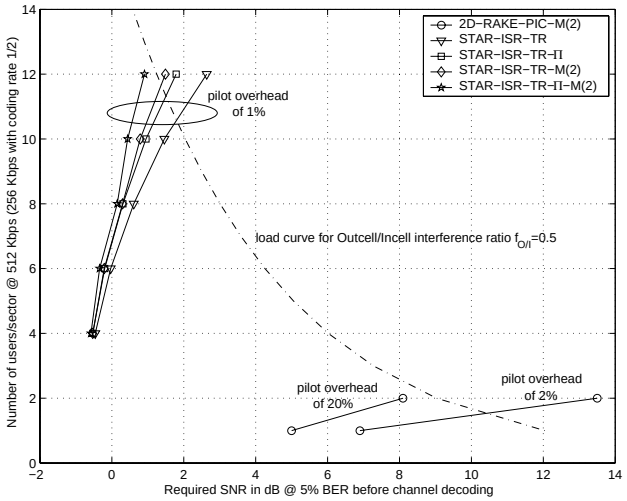

Fig. 2. Same as Fig. 1 with faster channel variations (*i.e.*, Doppler spread of 106 Hz at 60 Kmph and delay drift of 4 ppm.

L), a Doppler spread $f_D = 1.8$ Hz (*i.e.*, 1 Kmph), and a delay drift of 0.046 ppm (see [1],[2] for specification of other simulation parameters). We assess performance in terms of required SNR at a BER of 5% before FEC decoding versus the number of users per cell or per sector (*i.e.*, cell or sector load) and find the maximum capacity achievable below the load curve (see dashed line in Figs. 1 and 2) for an outcell to incell interference ratio $f_{O/I} = 0.5$ [1].

In Fig. 1, the four HDR versions of the STAR-ISR receiver accommodate 12, 13, 13 and 14 HDR terminals per cell or per sector, respectively, while the 2D-RAKE-PIC cannot accommodate more than 3 terminals at the same complexity [1],[2]. These results confirm the advantages of the new block Π-DFI procedure and the multistage option [1] and suggest capacity and spectrum efficiency gains of STAR-ISR-TR over the 2D-RAKE-PIC by as much as a factor 4 to 5. With fast channel variations in Fig. 2, STAR-ISR loads reduce to 10, 11, 11 and 12 terminals per cell or per sector, respectively. On the other hand, the 2D-RAKE-PIC cannot operate with 1% pilot-symbol overhead. With 2% overhead, it can accommodate one terminal only. For an overhead of 20% or higher, its capacity increases and saturates at a maximum of 2 terminals (*i.e.*, a useful information load of 1.6). Thus, in adverse channel conditions, the performance advantage of STAR-ISR-TR over the 2D-RAKE-PIC increases up to factor 6 in capacity and 7.5 in spectrum efficiency.

These results suggest that STAR-ISR offers a future upgrade path to greater capacities and faster data access with significant performance advantages over competing receiver solutions currently envisaged for implementation with equivalent complexity.

5. REFERENCES

[1] S. Affes, H. Hansen, and P. Mermelstein, "Interference subspace rejection: A framework for multiuser detection in wideband CDMA", *IEEE J. Selec. Areas Comm.*, vol. 20, no. 2, pp. 287-302, February 2002.

[2] K. Cheikhrouhou, S. Affes, and P. Mermelstein, "Impact of synchronization on performance of enhanced array-receivers in wideband CDMA networks", *IEEE J. Selec. Areas Comm.*, vol. 19, no. 12, pp. 2462-2476, December 2001.

[3] 3rd Generation Partnership Project, Technical Specification Group (TSG), Radio Access Networks (RAN), *Physical Layer Aspects of UTRA High Speed Downlink Packet Access*, 3GPP TR 25.848, V4.0.0, 2001.

[4] S. Affes, H. Hansen, and P. Mermelstein, "Interference subspace rejection in wideband CDMA: Modes for mixed-power operation", *Proc. of IEEE ICC'01*, 2001, vol. 2, pp. 523-529.

[5] Y.J. Guo, S. Vagdama, and Y. Tanaka, "Advanced base station technologies for UTRA", *Electronics & Communications Journal*, pp. 123-133, June 2000.

[6] M. Sawahashi, K. Higuchi, and F. Adachi, "Experiments on pilot symbol-assisted coherent multistage interference canceller for DS-CDMA mobile radio", *IEEE J. Selec. Areas Comm.*, vol. 20, no. 2, pp. 433-449, February 2002.

[7] S. Affes, H. Hansen, and P. Mermelstein, "Near-far resistant single-user channel identification by interference subspace rejection in wideband CDMA", *Proc. of IEEE SPAWC'01*, 2001, pp. 54-57.